

Arabidopsis COBRA-LIKE 10, a GPI-anchored protein, mediates directional growth of pollen tubes

Sha Li^{1,†}, Fu-Rong Ge^{1,†}, Ming Xu^{2,†}, Xin-Ying Zhao¹, Guo-Qiang Huang¹, Liang-Zi Zhou¹, Jia-Gang Wang¹, Anja Kombrink³, Sheila McCormick², Xian Sheng Zhang^{1,*} and Yan Zhang^{1,2,*}

¹State Key Laboratory of Crop Biology, College of Life Sciences, Shandong Agricultural University, Tai'an, 271018 Shandong, China,

²Plant Gene Expression Center, Agricultural Research Service, University of California-Berkeley and United States Department of Agriculture, Albany, 94710 CA, USA, and

³Phytopathology, Wageningen University, Wageningen 6708 PB, The Netherlands

Received 15 October 2012; revised 29 January 2013; accepted 31 January 2012; published online 6 February 2013.

*For correspondence (e-mail yzhang@sdau.edu.cn or zhangxs@sdau.edu.cn)

†These authors contributed equally to this work.

SUMMARY

Successful reproduction of flowering plants requires constant communication between female tissues and growing pollen tubes. Female cells secrete molecules and peptides as nutrients or guidance cues for fast and directional tube growth, which is executed by dynamic changes of intracellular activities within pollen tubes. Compared with the extensive interest in female cues and intracellular activities of pollen tubes, how female cues are sensed and interpreted intracellularly in pollen is poorly understood. We show here that COBL10, a glycosylphosphatidylinositol (GPI)-anchored protein, is one component of this pollen tube internal machinery. Mutations in *COBL10* caused gametophytic male sterility due to reduced pollen tube growth and compromised directional sensing in the female transmitting tract. Deposition of the apical pectin cap and cellulose microfibrils was disrupted in *cobl10* pollen tubes. Pollen tube localization of COBL10 at the apical plasma membrane is critical for its function and relies on proper GPI processing and its C-terminal hydrophobic residues. GPI-anchored proteins are widespread cell sensors in mammals, especially during egg-sperm communication. Our results that COBL10 is critical for directional growth of pollen tubes suggest that they play critical roles in cell-cell communications in plants.

Keywords: glycosylphosphatidylinositol-anchored protein, polar growth, asymmetric localization, wall organization, cell-cell communication.

INTRODUCTION

Double fertilization of flowering plants has been a fascinating research area for over a century. It is a process in which two immotile sperm cells carried within a pollen tube fertilize two female gametes, the egg and the central cell, to form the embryo and endosperm respectively (McCormick, 1993). After pollen lands on compatible stigmatic cells and germinates, pollen tubes grow deep inside pistils, penetrating different parts of the female tissues to arrive precisely at the micropyle of the ovule and deliver sperm (Cheung *et al.*, 2010). Unlike most plant cells, a pollen tube grows in a polar, rather than in a diffuse way, forming a cylindrically shaped cell. Pollen tubes can grow *in vitro* when supplied with simple chemical ingredients but are able to achieve faster growth in the presence of female nutrients (Cheung *et al.*, 1995; Wu *et al.*, 2000; Tang

et al., 2004). In addition, female tissues release molecules or proteins to guide the directional growth of pollen tubes (Higashiyama *et al.*, 2001; Palanivelu *et al.*, 2003; Marton *et al.*, 2005; Palanivelu and Preuss, 2006; Chen *et al.*, 2007; Okuda *et al.*, 2009; Chae and Lord, 2011).

Polar growth is made possible through the dynamic maintenance of spatial asymmetry within pollen tubes. Elongating pollen tubes are structurally asymmetric. First, pollen tubes are composed of different intracellular zones defined by the presence of different organelles and distinct actin cytoskeletal structures (Cheung and Wu, 2007). Second, the cell wall of pollen tubes is organized differentially. That is, the pollen tube wall has a spatially distinct organization such that the apical wall consists mostly of a methylated pectic layer allowing cell expansion, while the shank

wall is mostly made from demethylated pectin, whose rigidity maintains tube morphology and represses lateral growth (Geitmann, 2010). Third, the plasma membrane of pollen tubes is asymmetrical, such that signaling proteins or molecules are distributed in a spatially restricted manner (Benedikt, 2008), and in a way that resembles metazoan chemotactic cells in which signaling molecules such as Rac GTPases and phosphoinositides are distributed differentially either at the cell front or back for attractant sensing and directional movement (Kolsch *et al.*, 2008).

To reach their precise targets, pollen tubes communicate with female cells along their path and adjust their growth axis in response to female cues (Johnson and Preuss, 2002; Cheung *et al.*, 2010). However, compared with extensive studies on the identity of female cues as well as dynamic changes of intracellular activities within pollen tubes, little progress has been made in the identification of sensors in pollen tubes that perceive female cues and interpret them into dynamic changes of growth asymmetry.

Glycosylphosphatidylinositol (GPI)-anchored proteins (GPI-APs) are potential cell sensors in eukaryotes. GPI-APs generally consist of an N-terminal signal peptide (SP) for secretion, a hydrophilic middle region and a hydrophobic C-terminal SP for GPI processing and membrane anchoring (Chatterjee and Mayor, 2001; Ikezawa, 2002). GPI-APs are synthesized in the lumen of the endoplasmic reticulum (ER) via the sequential addition of monosaccharides, fatty acids, phosphoethanolamines and phosphatidylinositol (PI) (Ikezawa, 2002; Lalanne *et al.*, 2004). Processed proteins are secreted from the ER and finally are anchored at the outer leaflet of the plasma membrane (PM). Some GPI-APs are further processed through proteolysis and released in the extracellular space (Ikezawa, 2002). Because the cell surface is the first region through which cells sense and respond to the environment, GPI-APs are likely candidates to perform such functions.

That GPI-APs play roles in pollen tube growth was suggested by genetic studies of GPI-AP-processing enzymes in Arabidopsis. The first processing step of GPI-APs at the ER was catalyzed by a GPI-N-acetylglucosaminyltransferase (GPI-GnT) complex that consists of at least six subunits in Arabidopsis, two of which regulate pollen tube growth. Mutations at *SETH1* and *SETH2*, encoding the PIG-C and the PIG-A subunit of the GPI-GnT complex respectively, caused defects in pollen germination and tube growth, leading to male gametophytic lethality (Lalanne *et al.*, 2004). Arabidopsis *PEANUT1* (*PNT1*), encoding a mannosyltransferase (PIG-M) for GPI-AP-processing, was also involved in pollen tube growth in that its mutations substantially reduced male gametophytic transmission (Gillmor *et al.*, 2005). Over 200 GPI-APs are encoded in the Arabidopsis genome (Borner *et al.*, 2003; Elortza *et al.*, 2003), dozens of which show pollen-specific or pollen-enriched expression patterns (Lalanne *et al.*, 2004). There-

fore, it was not known which GPI-APs contributed to the growth defects in *SETH1*, *SETH2* and *PNT1* loss-of-function mutants (Lalanne *et al.*, 2004; Gillmor *et al.*, 2005).

We show here that Arabidopsis *COBL10* controls female-guided fast and directional growth of pollen tubes probably by regulating the deposition of the apical pectin cap and cellulose microfibrils. *COBL10* belongs to the plant-specific *COBRA* family that encodes GPI-APs (Roudier *et al.*, 2002; Brady *et al.*, 2007). Members of the *COBRA* family mediate diverse cellular and developmental processes such as root growth (Schindelman *et al.*, 2001; Brown *et al.*, 2005; Roudier *et al.*, 2005), pathogen resistance (Ko *et al.*, 2006), stem strength (Li *et al.*, 2003; Sindhu *et al.*, 2007) and root-hair growth (Jones *et al.*, 2006; Hochholdinger *et al.*, 2008). Localization of *COBL10* at the pollen tube plasma membrane was restricted to the most apical region and is dependent on its C-terminal hydrophobic residues as well as on an intact PIG complex. Our results show that *COBL10* is an essential component of the internal machinery in pollen tubes that senses and interprets female signals.

RESULTS

COBL10 loss of function caused gametophytic male sterility

Three T-DNA insertion lines within the *COBL10* genomic region were available from Arabidopsis stock centers (Figure 1a). *cobl10-1* (CS876299) and *cobl10-2* (CS879411); both have insertions at the very end of the *COBL10* coding sequence. Transcript analysis (Figure 1b) and DNA sequencing indicated that although expression levels of *COBL10* in homozygous *cobl10-1* and *cobl10-2* mutants were equal to the expression level in wild type, the mutant transcripts potentially encode a *COBL10* whose last nine amino acids were replaced by an asparagine (Asn) residue due to the T-DNA insertion (Figure 1c). *cobl10-3* (CS875361) has a T-DNA inserted at the 3' untranslated (UTR) region; this mutant showed no transcriptional changes (Figure 1a,b) and was not analyzed further.

Homozygous plants of *cobl10* mutants were obtained at very low frequency from self-pollinated heterozygous plants (Table 1). No defects during vegetative growth were detected for homozygous *cobl10* mutants, as expected given its restricted expression pattern (Brady *et al.*, 2007). However, siliques of plants homozygous for either mutant allele were much shorter (Figure 1d–h), and contained on average four or five developing seeds in each silique (Figure 1i). Interestingly, these seeds were twice the size of the seeds from wild-type plants, mostly due to enlarged embryonic cells (Figure S1). Most ovules in siliques of homozygous *cobl10* mutants were tiny, and still contained the egg cell and central cell at 48 h after pollination (HAP) (Figure 1k), a time at which embryo developmental

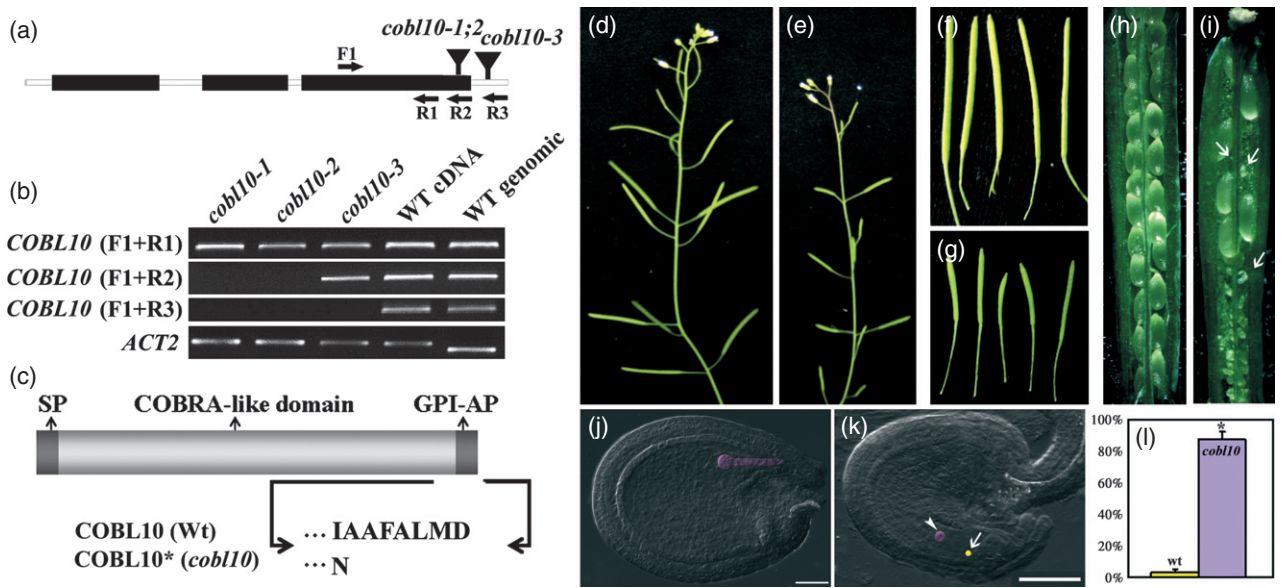


Figure 1. *COBL10* loss-of-function alleles exhibit male gametophytic sterility.

- (a) Schematic illustration of *COBL10* and its insertion mutants, and location of primers used in (b).
 (b) Transcript analysis for *COBL10* in wild type, *cobl10-1*, *cobl10-2*, and *cobl10-3*.
 (c) Domain organization of *COBL10*, highlighted with the C-terminal sequence in wild type (*COBL10*) or in mutants (*COBL10**). SP, N-terminal signal peptide; GPI-AP, C-terminal signal peptide for GPI-anchor.
 (d) Wild-type plant.
 (e) *cobl10-1* plant.
 (f) Representative mature siliques of wild type.
 (g) Representative mature siliques of *cobl10-1*.
 (h) Representative open silique of wild type.
 (i) Representative open silique of *cobl10-1*.
 (j) Wild-type ovule at 48 HAP. Developing embryo is colored pink.
 (k) Tiny *cobl10-1* ovule at 48 HAP. The central cell nucleus (arrowhead) is colored pink while the egg cell nucleus (arrow) is colored yellow.
 (l) Percentage of unfertilized ovules in siliques of wild type and *cobl10-1*. Data were collected from three independent experiments, each of which used five sequential siliques from 10 independent plants. Asterisk indicates significant difference (Student's *t*-test, $P < 0.01$). Scale bars for (j) and (k), 50 μ m.

Table 1 Loss of function of *COBL10* resulted in defective male transmission

Parent	F1 segregation	Expected	Observed ratio
Female X Male	Genotype		
<i>cobl10-1</i> +/- × <i>cobl10-1</i> +/-	<i>COBL10</i> +/+; +/-; -/-	1:2:1	100:126:7 ^a
<i>cobl10-1</i> +/- × WT	<i>COBL10</i> +/+; +/-	1:1	121:108 ^b
WT × <i>cobl10-1</i> /	<i>COBL10</i> +/+; +/-	1:1	130:3 ^c
<i>cobl10-2</i> +/- × <i>cobl10-2</i> +/-	<i>COBL10</i> +/+; +/-; -/-	1:2:1	76:92:4 ^a
<i>cobl10-2</i> +/- × WT	<i>COBL10</i> +/+; +/-	1:1	84:79 ^b
WT × <i>cobl10-2</i> +/-	<i>COBL10</i> +/+; +/-	1:1	93:2 ^c

^aSignificantly different from the segregation ratio 1:2:1 (Student's *t*-test, $P < 0.01$).

^bNot significantly different from the Mendelian segregation ratio (Student's *t*-test, $P > 0.05$).

^cSignificantly different from the segregation ratio 1:1 (Student's *t*-test, $P < 0.01$).

processes had already started in wild type (Figure 1j) and suggesting failed fertilization rather than defective embryo development.

To find out which gametophyte was defective, we performed reciprocal crosses between *cobl10* heterozygous mutants and wild type. The segregation ratios of progenies from these reciprocal crosses showed that mutant male gametophytes transmitted poorly while mutant female

gametophytes were normal (Table 1), even though *COBL10* was also expressed in ovules (Brady *et al.*, 2007).

***COBL10* is not essential for pollen development, hydration, or germination**

There are different stages at which the male gametophyte could be defective, i.e. pollen development, germination, polar and directional tube growth, and sperm delivery

(Johnson and Preuss, 2002). We therefore analyzed male gametophytes of *cobl10* at different stages to determine the reason for poor transmission (Methods S1). Pollen viability staining with 4',6-diamidino-2-phenylindole (DAPI) and Alexander's stain (Johnson-Brousseau and McCormick, 2004) showed no differences between wild type (Figure S2a) and *cobl10* (Figure S2(b)). Scanning electron micrographs (SEM) showed that the pollen coat of *cobl10* mutants (Figure S2(d)) was like that of wild type (Figure S2(c)). These results indicated that *cobl10* pollen developed normally.

Next, we tested whether pollen hydration and germination was affected in *cobl10* by analyzing pollen germination *in vitro* or on stigma. We introduced *quartet1* (*qrt*) and *Pro_{LAT52}:GUS* into *cobl10* to make scoring of germination more accurate. The *qrt1* mutant contains pollen tetrads instead of separate pollen grains and *Pro_{LAT52}:GUS* allows histochemical staining of pollen tubes growing both *in vitro* and *in vivo* (Johnson-Brousseau and McCormick, 2004). Homozygous *cobl10;qrt;Pro_{LAT52}:GUS* pollen showed no differences in germination percentage and growth speed, compared with *qrt;Pro_{LAT52}:GUS* as wild type (Figure S3a, d). Germination and hydration on the stigma was not also affected (Figure S2(f)). These results indicated that *COBL10* is not essential for pollen development, hydration, or germination.

Pollen tube growth in the transmitting tract is defective in *cobl10*

The distorted segregation ratios (Table 1) and near sterility of mutants (Figure 1) indicated that male transmission was disrupted in *cobl10*. Therefore, the lack of detectable defects for *cobl10* pollen at developmental stages as well as during germination implied defects late in male gametophyte function, i.e. pollen tube growth. We therefore examined whether pollen tube growth was affected in *cobl10*. Surprisingly, no defects in germination, morphology and growth speed were detected for *cobl10* pollen tubes growing *in vitro* (Figure S3).

We next examined pollen tube growth in pistils by histochemical analysis of emasculated wild-type pistils hand-pollinated with either *cobl10;qrt;Pro_{LAT52}:GUS* or *Pro_{LAT52}:GUS* pollen (WT). At 9 hours after pollination (HAP), WT pollen tubes reached the bottom of the pistil and most ovules were targeted by a pollen tube (Figure 2a). In comparison, *cobl10* pollen tubes were slower (Figure 2b). We performed an additional time course analysis of pollen tube growth *in vivo* by analyzing pistils at progressive time points to determine in which female tissue(s) the growth of *cobl10* pollen tubes slowed down. Pistils pollinated by *cobl10* pollen at 0.5 HAP and 1.5 HAP showed a growth front of most of the tubes at the stigma and style, respectively (Figure 2b), similar to wild type (Figure 2a). However, *cobl10* pollen tubes grew slower than those of wild

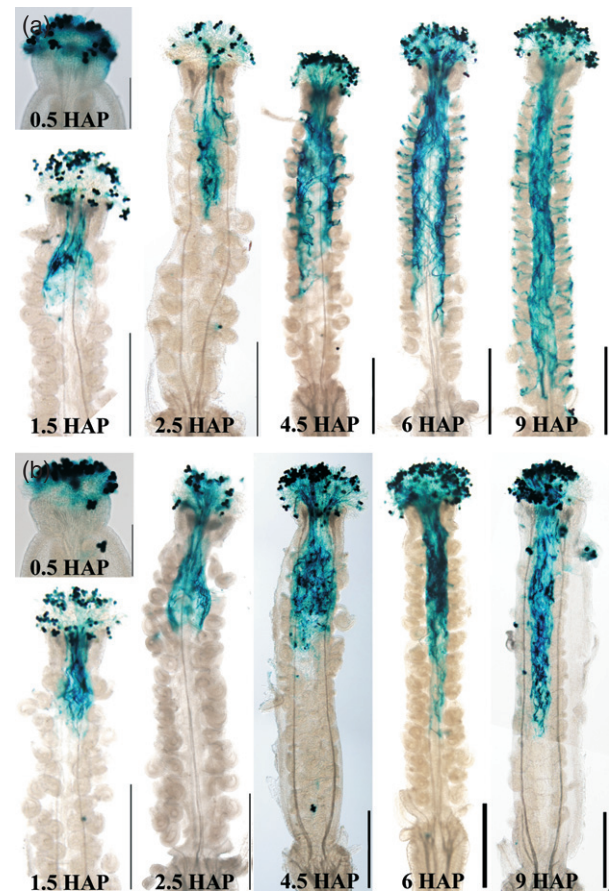


Figure 2. Pollen tube growth of *cobl10* is reduced in the transmitting tract. (a) Representative histochemical staining of *Pro_{LAT52}:GUS* pollen on emasculated wild-type pistils at 0.5, 1.5, 2.5, 4.5, 6, or 9 HAP. (b) Representative histochemical staining of *cobl10;qrt;Pro_{LAT52}:GUS* on emasculated wild-type pistils at 0.5, 1.5, 2.5, 4.5, 6, or 9 HAP. Images shown are representative of three independent experiments. Seven or eight pistils were analyzed at each time point in each experiment. Except for pistils at 2.5 h whose scale bars represent 200 μ m, scale bars represent 500 μ m.

type at time points from 2.5 HAP onwards, when the growth front of most WT tubes were in the transmitting tract, the so-called 'pollen tube superhighway' (Johnson and Preuss, 2002; Figure 2b).

Pollen tubes of *cobl10* are hyposensitive to ovule guidance cues

In addition to reduced tube growth, pollen tubes of *cobl10* were less likely to turn toward the micropyle (Figure 3a–d). Indeed, only a few ovules were targeted by *cobl10* pollen tubes, even though the pollen tubes did reach the bottom of pistils at 48 HAP (Figure 3a–d), and suggesting a compromised ability to respond to ovular guidance signals.

To provide further evidence, we used a semi-*in vivo* pollen tube guidance assay (Palanivelu and Preuss, 2006), which assesses the ability of pollen tubes to sense ovular signals after emerging from the stigma and style, and thus

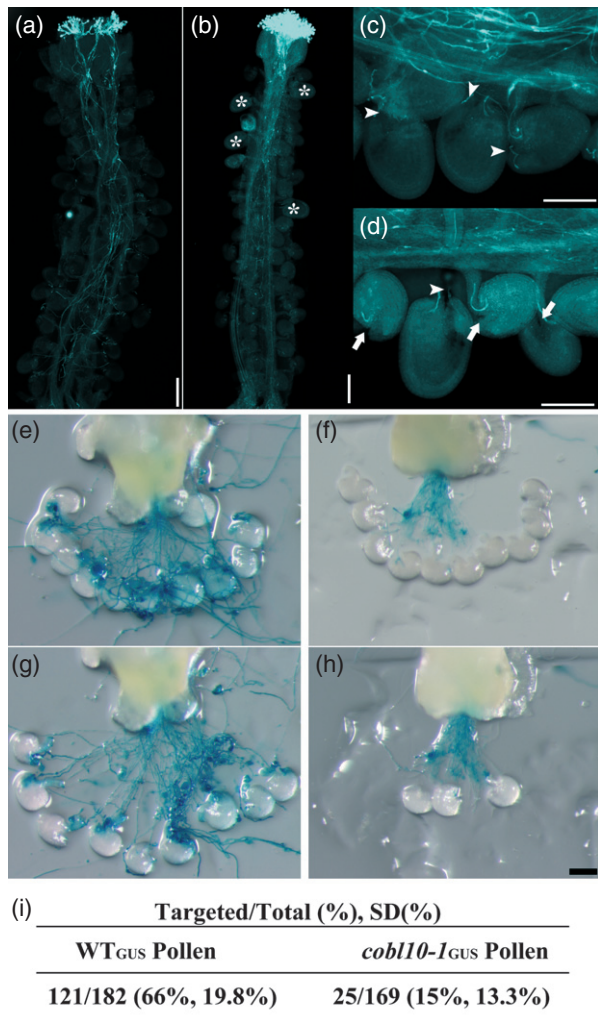


Figure 3. Compromised directional growth of *cob110* pollen tubes. Aniline blue staining of wild-type pollen (a) or *cob110* pollen (b) on emasculated wild-type pistils at 48 HAP. Asterisks indicate fertilized ovules by *cob110* pollen. Close-up images of pistils targeted by wild-type pollen (c) or by *cob110* pollen (d) show compromised tube turning in *cob110* despite the available pollen tubes in the transmitting tract. Semi-*in vivo* pollination assays (e–h). Because untargeted ovules can float away while targeted ovules are connected by penetrating tubes after gentle washing, each experiment was photographed before (e,g) and after gentle washing (f,h) for wild type (e,f) and *cob110* mutants (g,h). (i) Targeting efficiency, i.e. number of targeted ovules to total ovules of wild type or *cob110* pollen. Arrows indicate micropyle not targeted by a pollen tube while the arrowheads point at micropyle targeted by a pollen tube. Images shown in (a,b) are representative of 20–30 pistils analyzed. Results of the semi-*in vivo* assay are from 18 independent experiments. Around 10 ovules from unfertilized pistils were placed in front of cut ends of styles pollinated with either wild type (e,f) or *cob110* pollen (g,h) in each experiment. SD, standard deviation. Scale bars for (c) and (d), 200 μm , for (e) to (h), 100 μm .

is not influenced by female components in the transmitting tract. Our previous results showed that *COBL10* was required for pollen tube *in vivo* growth primarily in the transmitting tract. Therefore, the semi-*in vivo* system would exclude the possibility that reduced growth of *cob110* pollen tubes indirectly affected its tube turning and

would reflect the ability of *cob110* pollen tubes to sense guidance cues from the ovule. Both wild type (WT_{GUS}) (Figure 3e) and *cob110*_{GUS} (Figure 3f) pollen tubes grew out from cut styler ends on germination medium. However, pollen tubes of WT_{GUS} grew toward all ovules located in front of the styles in a circle (Figure 3e,g), while pollen tubes that targeted *cob110*_{GUS} were compromised (Figure 3f,h). Over 60% of the ovules were targeted by a wild-type pollen tube, whereas <20% were targeted by a *cob110* tube (Figure 3i), a finding that indicated severely compromised signal sensing of *cob110* pollen tubes.

***cob110* pollen tubes growing *in vivo* had abnormal cell wall organization**

Because mutations at other *COBs* were reported to affect dynamic cell wall organization (Roudier *et al.*, 2002; Li *et al.*, 2003; Brown *et al.*, 2005; Sindhu *et al.*, 2007; Hochholdingner *et al.*, 2008), we wondered if *cob110* mutants would be similar. We first examined the cell wall in pollen tubes growing *in vitro* using histochemical stains. Aniline blue stains callose, calcofluor white stains both cellulose and callose, and ruthenium red stains pectin (Lalanne *et al.*, 2004; Wang *et al.*, 2011). In growing pollen tubes, calcofluor white stained uniformly along the pollen tube wall, with a slightly higher intensity along the shank than at the apical region, both in wild type (Figure S4a) and *cob110* (Figure S4(b)). Both wild-type and *cob110* tubes showed an apical pectin cap as well as a weak pectin signal along the tube shank (Figure S4(c,d)). Aniline blue stained the apical region, tube shank and callose plugs comparably in wild type and *cob110* (Figure S4e,f). That no staining differences for all three carbohydrate groups was detectable between wild type and *cob110* pollen tubes growing *in vitro* (Figure S3) correlated with the normal growth of *cob110* pollen tubes *in vitro*.

Because *cob110* pollen tubes grew more slowly than those of wild type only in the transmitting tract (Figure 2), its potential effects on wall organization would be seen only when growing *in vivo*. We first analyzed the distribution of pectins in pollen tubes growing out of the styles in the semi-*in vivo* experiments in which we did observe a slight reduction in tube growth in *cob110*. As shown in Figure 5, we could clearly see the difference by JIM7 labeling between wild type and mutants. Instead of concentrating at the apical region in wild type (Figure 5a), in *cob110* JIM7 labeling was evenly spread to the whole tube wall (Figure 5b). JIM5 that labels de-esterified pectins (Chebli *et al.*, 2012) did not show any marked difference between wild type and *cob110*, such that JIM5 labeling was strongest along the shank wall but weakest at the apical wall in both genetic backgrounds. Considering that pollen tubes from both genotypes had been given the same treatments and captured using the same gain value in confocal imaging, the only difference between wild type and *cob110* by JIM5

labeling is that the signal intensity was stronger in *cobl10* tubes (Figure 5d) than in the wild-type tubes (Figure 5c).

We therefore used transmission electron micrograph (TEM) to determine whether *cobl10* pollen tubes had a defective wall structure *in vivo*, using wild-type pistils pollinated with either wild-type or *cobl10* pollen for 4 h. Wild-type tubes growing in pistils had a very distinct spatial wall structure such that a thick layer of a porous cap was at the apical dome and dense fibrous cellulose was at the shank wall (Figure 4a–c). In contrast, in *cobl10* pollen no apparent apical cap was detected (Figure 4d,e), and the shank walls

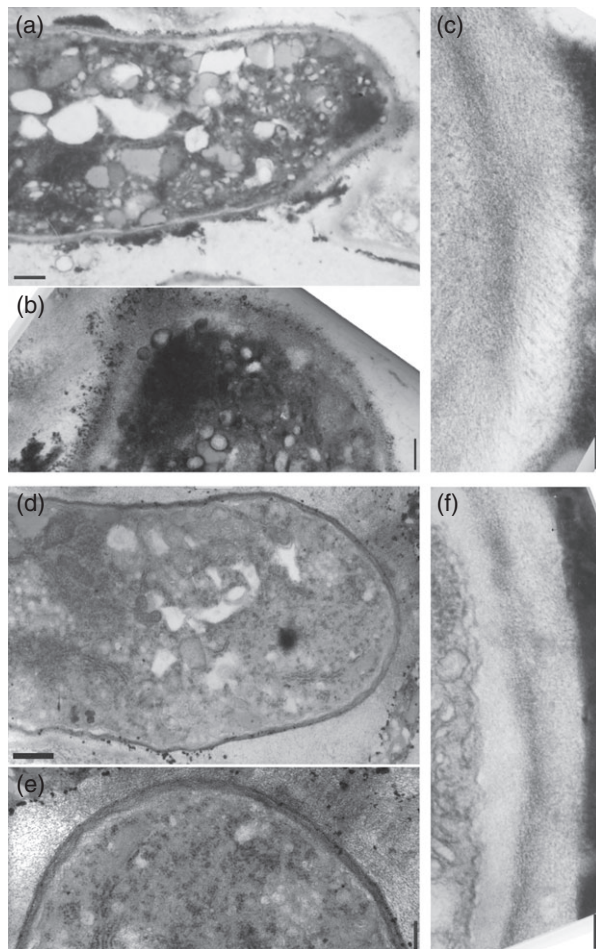


Figure 4. *cobl10* pollen tubes growing *in vivo* lack a pectin cap and have reduced cellulose microfibrils. (a) The tip of a wild-type pollen tube. (b) Close-up at the apical region of the pollen tube in (a), showing a pectin cap. (c) Shank wall of wild-type pollen tube showing the deposition of cellulose microfibrils. (d) A *cobl10* pollen tube. (e) Close-up at the apical region of the pollen tube in (d), showing absence of a pectin cap. (f) Shank wall of *cobl10* pollen tube. Note the absence of cellulose microfibrils. Images shown are representatives of transmission electron micrographs (TEMs) performed from six fixed pistils prepared from three independent experiments. More than five individual pollen tubes were captured by TEM in each fixed sample. Scale bars for (a,d), 500 nm; for (b,e), 200 nm; for (c,f), 100 nm.

contained no detectable fibrous cellulose (Figure 4f), such that spatial information regarding cell wall organization was lost. Considering the pollen tube growth defects of *cobl10*, that *cobl10* pollen tubes had defective cell wall organization *in vivo* but not *in vitro* suggested that *COBL10* functions only in the presence of female nutrients and regulatory cues.

Asymmetric localization of *cobl10* at the plasma membrane

GPI-anchors often serve as a signal for polar protein sorting in metazoan cells such as neutrophils and epithelial cells (Chatterjee and Mayor, 2001), to which pollen tubes show a certain mechanistic resemblance. Therefore, we wondered about the subcellular localization of *COBL10*. Because GPI-APs contain both N- and C-terminal signal peptides and because protein fusions at either end would interfere with their processing and targeting, we generated *ProCOBL10*:SP-citrine-COBL10 in which the coding sequence of a pH-insensitive yellow fluorescent protein (YFP) variant (citrine) (Tian *et al.*, 2004) was inserted in-frame behind the N-terminal SP coding sequence of the *COBL10* genomic sequence. Introduction of this construct into *cobl10* rescued the fertility defect fully, as shown by *COBL10*-citrine expression (Figure 6a) and fully elongated siliques

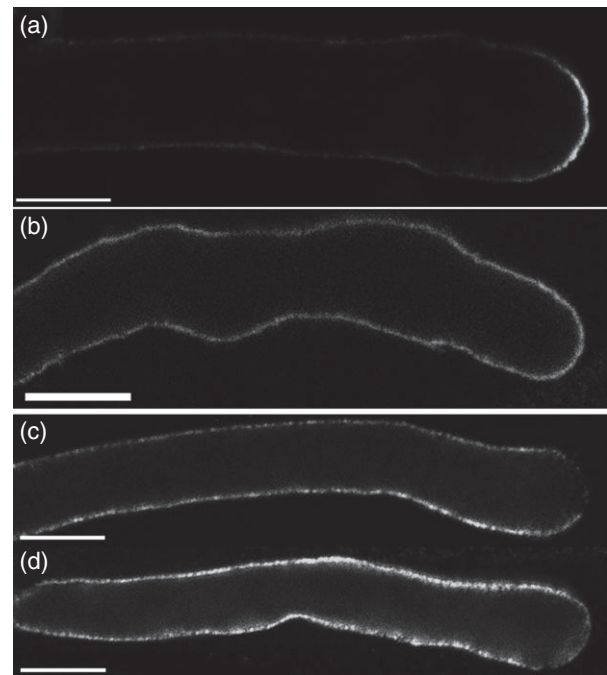


Figure 5. Immunofluorescence labeling of pectins in semi-*in vivo* pollen tubes. Fluorescence micrographs of median optical sections of wild-type tubes (a,c) or *cobl10* tubes (b,d). Immunofluorescence label was performed using antibody JIM7 for highly esterified pectins (a,b) or JIM5 for de-esterified pectins (c,d). (c) and (d) show images taken at the same gain value for comparison purposes. Representative tubes of three replicate experiments involving 20–30 pollen tubes are shown for each treatment. Scale bars, 7.5 μ m.

(Figure 6e), suggesting that the citrine fusion did not affect the function of COBL10.

Using *in vitro* pollen germination, we detected the citrine signal at a restricted region of the apical plasma membrane as well as in motile punctate vesicles (Figure 6a). Although fairly weak, the apical plasma membrane localization of COBL10 was dynamically maintained during tube growth (Movie S1). To determine the identity of the punctate vesicles containing COBL10, we used pharmacological treatment on transgenic pollen tubes. Brefeldin A (BFA) inhibits trafficking of vesicles secreted from the *trans*-Golgi network (TGN)/early endosome (EE), while wortmannin (WM) inhibits the production of PI3P and therefore aggregates certain populations of endosomes in pollen tubes (Zhang *et al.*, 2010). BFA did not cause aggregation of the punctate vesicles of COBL10 but abolished its apical PM localization (Figure 6b), suggesting that COBL10 at the apical plasma membrane was delivered by an ArfGEF-dependent post-Golgi trafficking route (Jürgens, 2004). The COBL10 signal was detected at the 'BFA compartment' together with the lipophilic dye FM4-64 (Figure 6b). WM treatment caused aggregation of most vesicles as well as loss of the apical PM signal (Figure 6c), suggesting that the COBL10-resident vesicles had an endosome identity.

Localization of COBL10 at the apical plasma membrane depended on its C-terminal hydrophobic residues and an intact PIG complex

Studies of animal GPI-APs indicated that the C-terminal hydrophobic residues were critical for their correct processing or stability (Berger *et al.*, 1988; McDowell *et al.*, 1998). That *cobl10* potentially expressed a truncated COBL10 with the last nine amino acids missing, but still showed a mutant phenotype that was fully rescued by *COBL10*, suggested that the C-terminal hydrophobic residues were important. To determine whether the C-terminal hydrophobic residues were critical for the subcellular localization of COBL10, we generated *Pro*_{COBL10}:SP-citrine-COBL10ΔC9, which expressed a COBL10 version whose last nine amino acids were replaced with an Asn, mimicking the protein potentially expressed in *cobl10* mutants (Figure 1). Indeed, transgenic Arabidopsis pollen tubes that expressed SP-citrine-COBL10ΔC9 lost the apical plasma membrane signal (Figure 6d). Although punctate vesicles still were visible, a substantial signal was detected at filamentous structures (Figure 6d) similar to that of the ER (Cheung and Wu, 2007). To confirm the ER localization, we introduced calnexin-RFP, the ER marker (Gao *et al.*, 2012), into pollen tubes expressing COBL10ΔC9. Indeed, most of COBL10ΔC9 was colocalized with calnexin, indicating its ER localization (Figure S5). *Pro*_{COBL10}:SP-Citrine-COBL10ΔC9 could not rescue the sterility of *cobl10* (Figure 6e,f).

Although COBL10 was predicted to be a GPI-AP (Roudier *et al.*, 2002; Brady *et al.*, 2007), it was not experimentally tested. We reasoned that if COBL10 were indeed a GPI-AP, it would show different subcellular localization when the Arabidopsis PIG complex was not functional. To find out whether this was the case, we characterized mutant alleles of *SETH1* and *SETH2* (Lalanne *et al.*, 2004). The heterozygous *seth2* mutant showed pollen growth defects such that germination percentage was reduced and mutant pollen tubes ceased growth early as had been reported previously (Lalanne *et al.*, 2004). While a new mutant allele of *seth1*, *seth1-4* (Methods S1) showed similar pollen growth defects (Figure S5) as reported for the other *SETH1* alleles (Lalanne *et al.*, 2004). *Pro*_{COBL10}:SP-citrine-COBL10 was then introduced into *seth1-4* or *seth2* heterozygous mutants and the citrine signal was analyzed in transgenic pollen tubes. In most pollen tubes that showed the *seth1-4* or *seth2* phenotype (Lalanne *et al.*, 2004), the citrine signal was detected at the filamentous ER structure as well as at punctate vesicles, but not at the apical plasma membrane (Figure S5), similar to the results shown by COBL10ΔC9 (Figure 6d). This result indicated that processing of COBL10 by the PIG complex was critical for its subcellular localization.

Pollen-specific COBL11 confers partial redundancy to COBL10

That *cobl10* plants were still able to set a few seeds in each silique suggested functional redundancy. Indeed, *COBL11*, another member of the *COBL* family in Arabidopsis, is similar to *COBL10* and also expressed specifically in pollen (Brady *et al.*, 2007). We obtained two SAIL lines from ABRC (SAIL_326_A05 and SAIL_825_B08) that allegedly contained insertions in the *COBL11* genomic region. However, no T-DNA insertions could be identified by genotype analysis. To find out whether *COBL11* was functionally homologous to *COBL10*, we took a different approach by introducing a citrine-fused COBL11 into *cobl10* mutants. The subcellular localization of COBL11 resembled that of COBL10 at the apical plasma membrane and punctate vesicles (Figure S6b). *Pro*_{COBL11}:SP-Citrine-COBL11 in *cobl10* mutants partially rescued the reduced seed set (Figure S6a,c,d), a finding that suggested that *COBL11* plays a redundant, albeit less important function, than *COBL10*.

DISCUSSION

Considering the increasingly rich information on both sides of the sexual game, the question as to how pollen tubes perceive female cues and translate them into coordinated cellular activities requires more attention. Genes whose mutations show defective male gametophytic function only in the presence of female signals are keys that link extracellular guidance cues to intracellular networks that define and reorient the growth of pollen tubes. Many

mutants have defects in polarized growth of pollen tubes *in vitro*, without input from the female (Fu *et al.*, 2001; Fritsch *et al.*, 2007; Sousa *et al.*, 2008; Szumlanski and Nielsen, 2009; Ye *et al.*, 2009; Zhang *et al.*, 2009; Wang *et al.*, 2011), suggesting that they affect components of the pollen tube internal machinery. Although such components might also participate in cellular changes during female-guided growth, it is difficult to separate their functions in maintaining polar growth from responding to female cues. The expression of *COBL10* is high in mature pollen grains and in tubes growing *in vitro* and *in vivo* (Honys and Twell, 2004; Brady *et al.*, 2007; Qin *et al.*, 2009). The semi-*in vivo* assays (Figure 3) showed that pollen tubes of *cobl10* are severely compromised in female-guided growth. This finding is supported by the near sterility of *cobl10*. The increased seed size in *cobl10* (Figure S1) might be because more resources were allocated to the few fertilized ovules in each silique.

The only other mutants reported to date that specifically showed guidance defects were mutated at genes that encode two potassium transporters (Lu *et al.*, 2011) and *POD1* (Li *et al.*, 2011). However, the ER localization of the K⁺ transporters and *POD1* (Li *et al.*, 2011; Lu *et al.*, 2011) suggests indirect signal sensing. In comparison, *COBL10* functions at the apical plasma membrane of pollen tubes. In addition to previous predictions (Roudier *et al.*, 2005; Brady *et al.*, 2007) and results of proteomic studies (Borner *et al.*, 2003; Elortza *et al.*, 2003, 2006) suggesting that COBs are GPI-APs, we show that *COBL10* lost its apical plasma membrane localization in *seth1* and *seth2* mutants (Figure S5), a result that strongly supports the idea that *COBL10* is a GPI-AP. GPI-APs play critical roles in mammalian cell–cell communication (Chatterjee and Mayor, 2001; Ikezawa, 2002), especially important in fertilization, as mutations of GPI-APs expressed either in eggs (Alfieri *et al.*, 2003; Primakoff and Myles, 2007) or in sperm (Kondoh *et al.*, 2005) prevented fertilization. Comparable with the intense communication between egg and sperm in mammals, interactions between pollen tubes and female tissues are critical for fertilization in flowering plants. It was recently reported that *LORELEI*, a GPI-AP expressed in female gametophytes, is critical for communication with incoming pollen tubes during pollen tube reception (Capron *et al.*, 2008; Tsukamoto *et al.*, 2010). We showed that *COBL10* at the apical plasma membrane of pollen tubes mediates perception or interpretation of female signals, suggesting that GPI-APs have been adopted as key determinants of fertilization during evolution, even though different phyla use divergent regulatory mechanisms.

The specific role of *COBL10* during signal perception and interpretation probably involves dynamic organization of the pollen tube wall. Studies of other COB members have indicated that COBs affect cell wall organization (Li *et al.*, 2003; Roudier *et al.*, 2005; Ching *et al.*, 2006; Sindhu

et al., 2007; Hochholdinger *et al.*, 2008). We show here that mutations at *COBL10* disrupted the formation of the apical pectin cap as well as reduced the deposition of cellulose microfibrils along the tube shank (Figure 4). Such effects on carbohydrate deposition occur *in vivo* (Figure 4) but not *in vitro* (Figure S3), suggesting that *COBL10* function relies on the presence of female signals. The reduced tube growth of *cobl10* seen *in vivo* and the localization of *COBL10* at punctate vesicles as well as the plasma membrane are consistent with the idea that *COBL10* regulates cell wall synthesis or delivery of wall materials to the outside. The defects in tubes length *in vivo* also suggest that *COBL10* might have a role in sensing and relaying female cues needed to stimulate tube growth in the transmitting tract. However, we could not exclude the possibility that the insensitivity of *cobl10* pollen tubes to ovular guidance is an indirect outcome of compromised tip growth due to its inability to control wall modifications.

How *COBL10* regulates the cell wall organization of pollen tubes upon sensing female signals remains to be understood. One hypothesis involves pectin modifications. Methyl-esterified pectins are deposited at the apical cap of pollen tubes by inhibiting PME activity, maintaining the elasticity of the apical cap and thereby facilitating polar growth (Geitmann, 2010). COBs contain putative carbohydrate binding domains (CBD). It was reported that CBDs released by bacteria regulate plant PMEs to facilitate their entry into host cells (Hewezi *et al.*, 2008). Analogous to this mechanism during a plant–pathogen interaction, the CBD of *COBL10* may play similar roles during pollen–pistil interaction. Indeed, an *in silico* co-expression analysis (Obayashi *et al.*, 2011) showed that *COBL10* is found with both PME inhibitors and pectin lyases. A likely scenario to be explored in the future is that *COBL10* at the apical plasma membrane recruits or activates PME inhibitors and similar enzymes upon sensing female cues.

In animals, GPI-APs are processed at the ER by the PIG complex and transported via post-Golgi vesicles to the plasma membrane. Proper GPI processing relies on the C-terminal hydrophobic residues whose truncations caused either ER retention or protein degradation (Berger *et al.*, 1988; Fujita and Kinoshita, 2012; Galian *et al.*, 2012). We show here that localization of *COBL10* at the apical plasma membrane also relies on the C-terminal hydrophobic motif and proper GPI processing, suggesting an evolutionary conservation of GPI-AP targeting. Results from pharmacological treatments indicate that *COBL10* is present at post-Golgi vesicles (Figure 6), probably serving as trafficking vehicles for its final delivery.

Considering the dynamic feature of pollen tube growth, how the restricted localization of *COBL10* at the plasma membrane is maintained remains to be understood. In animal cells, GPI-APs are enriched at lipid rafts, which aggregate at the growth front of polarized cells (Gomez-Mouton

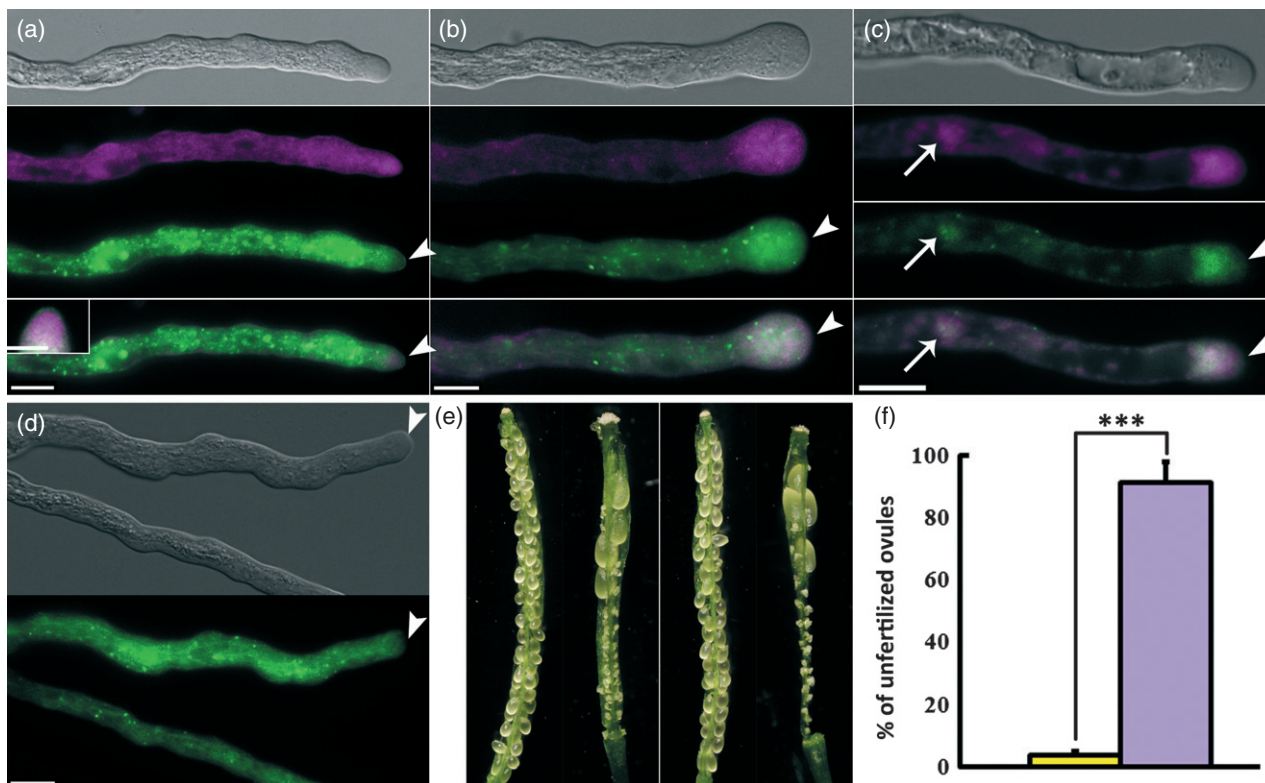


Figure 6. Apical plasma membrane localization of COBL10 relies on its C-terminal hydrophobic residues and is critical for its functionality. For (a), (b) and (c), from top to bottom are bright-field images, FM4-64 as shown in magenta, COBL10-citrine as shown in green and merge of the two fluorescent images. (a) Inset shows a magnified apical region of the pollen tube showing in (a). For (d), the bright-field image is in the top panel and citrine is in the bottom panel. Bars, 10 μm . Bar for (a) inset, 5 μm . (a) COBL10-citrine in wild-type tubes treated with FM4-64 for 5 min. Arrowheads indicate regions of the apical plasma membrane. (b) COBL10-citrine in wild-type tubes treated with FM4-64 for 5 min followed with 0.4 $\mu\text{g}/\mu\text{l}$ brefeldin A (BFA) for 30 min. Arrowheads indicate regions of the apical plasma membrane. (c) COBL10-citrine in wild-type tubes treated with FM4-64 for 5 min followed with 0.8 μM wortmannin (WM) for 1 h. Arrowheads indicate regions of the apical plasma membrane. Arrows indicate membranous aggregates caused by WM treatment. (d) COBL10 Δ C-citrine in wild-type tubes. Arrowheads indicate regions of the apical plasma membrane. (e) From left to right, representative siliques from a wild-type plant, a homozygous *cobl10* mutant, a homozygous *cobl10* mutant transformed with *ProCOBL10*:SP-citrine-COBL10, and a homozygous *cobl10* mutant transformed with *ProCOBL10*:SP-citrine-COBL10 Δ C9, respectively. (f) Percentage of unfertilized ovules in siliques of *cobl10* transformed with either *ProCOBL10*:SP-citrine-COBL10 (yellow bar) or *ProCOBL10*:SP-citrine-COBL10 Δ C9 (lilac bar). Data were collected with 50 siliques from 10 independent plants for each sample. Asterisks indicate significant difference (Student's *t*-test, $P < 0.01$).

et al., 2004). Pollen tubes, such as animal chemotactic cells, may also contain lipid rafts at the very apical region. Indeed, an alternate hypothesis for the specific function of COBL10 is that it could regulate the clustering of lipid rafts, which serve as signaling platforms to integrate multiple proteins for sensing or interpreting female cues during pollen–pistil interactions.

EXPERIMENTAL PROCEDURES

Plant growth and phenotype analysis

Arabidopsis plants were grown in a 4:1:1 mix of Fafard 4P:perlite:vermiculite under an 18-h light/6-h dark cycle at 21°C. T-DNA insertion lines including CS876299 (*cobl10-1*), CS879411 (*cobl10-2*), CS875361 (*cobl10-3*) and the alleged *COBL11* mutant alleles (SAIL_326_A05 and SAIL_825_B08) were obtained from the Arabidopsis Biological Resource Center (ABRC, Ohio State University).

The Col-0 *quartet1-2* (*qrt1*) mutant or *qrt1*;*ProLAT52*:GUS was used as wild type. Stable Arabidopsis transformation was done with the floral dipping method (Clough and Bent, 1998). Transgenic plants were selected on Murashige and Skoog medium supplemented with 30 mg/mg Basta salt (Sigma, <http://www.sigmaaldrich.com>). Ovules from 48 HAP pistils were incubated in Hoyer's solution for 45 min at 4°C, then cleared at room temperature for 2 h before visualization.

The segregation ratio of progenies from *cobl10* heterozygous plants or from reciprocal crosses was determined by polymerase chain reaction (PCR) analysis using the following primers: G1/G2 for *COBL10*, G2/G3 for *cobl10-1*, *cobl10-2* and *cobl10-3*. RNA extraction was performed with Qiagen RNeasy Plant Mini Kit (Qiagen, www.qiagen.com) according to the manufacturer's instruction. OligodT-primed cDNA was synthesized using SuperscriptTM III Reverse Transcriptase with on-column DNase treatment, as recommended by the manufacturer (Invitrogen, www.invitrogen.com). Primers used to characterize three *COBL10* mutants were F1, R1, R2 and R3. Primers used in reverse transcription (RT)-PCR

for endogenous *COBL10* were R4/R5; for exogenous *COBL10* were R6/R7. Primers are listed in Table S1. Primers to amplify *ACTIN2* (*ACT2*) are described in Zhang and McCormick (2007).

Plasmid construction

All constructs were generated using the Gateway™ technology (Invitrogen). The entry vector for *ProCOBL10*:SP-Citrine-COBL10 was generated according to a three-step PCR protocol described previously (Tian *et al.*, 2004) with primers P1/P2/P3/P4 and the citrine-specific primer pair P5/P6. The entry vectors for *ProCOBL10*:SP-citrine-COBL10ΔC9 were generated with primers P1/P7 using the full length *COBL10* entry vector as the template. The entry vector for *ProCOBL11*:SP-citrine-COBL11 was generated with primers P9/P10/P11/P12 and the citrine-specific primer pair P5/P6. The entry vector for calnexin was generated with primers P13/P14 using inflorescence cDNA as the template. Expression vectors were generated by LR reactions using LR Clonase II (Invitrogen, www.invitrogen.com) with a previously described Gateway destination vector (Zhang and McCormick, 2007). Primers are listed in Table S1.

All PCR amplifications used Phusion™ hot start high-fidelity DNA polymerase with the annealing temperature and extension times recommended by the manufacturer (Finnzyme). All entry vectors were sequenced using an ABI 3300 sequencer and sequences were analyzed using Vector NTI (Invitrogen). The Bioneer® PCR purification kit and Bioneer® Spin miniprep kit were used for PCR-product recovery and plasmid-DNA extraction, respectively.

Transmission electron micrograph

For sample fixation, four HAP wild-type pistils pollinated with either wild-type pollen or with *cobl10* pollen were treated according to the protocol for SEM. Tissues were then treated twice with propylene oxide for 2 h, propylene oxide:EPO812(1:1) (SPI-Chem™) for 12 h, EPO812 for 12 h, EPO812 for 24 h, and EPO812 + DMP-30 for 12 h. Samples were then fixed at 36°C for 12 h, at 45°C for 12 h, 60°C for 48 h. Fixed samples were sectioned with RM2265 (Leica, www.leica.com) to locate pollen tubes, then sectioned with Super Nova (Leica) for super-thin sections. Slides were stained with 2% uranyl acetate for 15 min, then lead citrate for 2 min and observed with a JEM-1200EX transmission electron microscope.

Immunofluorescent labeling of semi-*in vivo* pollen tubes

Semi-*in vivo* pollen tube growth was done as described (Palanivelu and Preuss, 2006). Immunofluorescent labeling was performed with JIM5 and JIM7 as well as CCRC-M1 as described (Chebli *et al.*, 2012).

Imaging

Microscopic imaging was performed using a dissecting scope (Leica), or Axio Observer D1 microscope (Zeiss, www.zeiss.com) with either bright-field, differential interference contrast (DIC) or epifluorescence optics, or with LSM780 laser scanning confocal microscope (Zeiss). Images were captured using a Spot digital camera (Diagnostic Instruments, http://www.diaginc.com/), exported using AXIOVISION software (Zeiss), and processed using Adobe Photoshop 7.0 (Adobe).

ACKNOWLEDGEMENTS

We thank the ABRC (<http://www.arabidopsis.org>) for the T-DNA insertion lines, Dr Li-Qun Chen from the Chinese

Agricultural University for help with immunofluorescent labeling of semi-*in vivo* pollen tubes and Dr Yi-Hua Zhou from the Institute of Genetics and Developmental Biology for the antibodies used in immunofluorescent labeling. This research was supported by the Major Research Plan (2013CB945100) from the Ministry of Science and Technology of China and by a grant from NSFC (31271578), and by the United States Department of Agriculture Current Research Information System to SM (grant no. 5335-21000-030-00D). YZ's laboratory and XZ's laboratory are supported by the Tai-Shan Scholar program from Shandong Provincial Government. The authors declare that there is no conflict of interest.

SUPPORTING INFORMATION

Additional Supporting Information may be found in the online version of this article.

Figure S1. *cobl10* has larger seeds than wild type due to increased embryonic cell size.

Figure S2. *cobl10* has normal pollen development, hydration and germination.

Figure S3. *cobl10* pollen showed normal germination and growth *in vitro*.

Figure S4. Pollen tubes of *cobl10* did not differ from those of wild type in carbohydrate deposition *in vitro*.

Figure S5. COBL10ΔC-citrine relocalized to the endoplasmic reticulum.

Figure S6. The apical plasma membrane localization of COBL10 relies on an intact PIG complex.

Figure S7. COBL10 function is partly redundant with COBL11.

Table S1. Primers used in this study.

Movie S1. Pollen tubes expressing SP-Citrine-COBL10 during *in vitro* growth.

Methods S1. Supporting experimental procedures.

REFERENCES

- Alfieri, J.A., Martin, A.D., Takeda, J., Kondoh, G., Myles, D.G. and Primakoff, P. (2003) Infertility in female mice with an oocyte-specific knockout of GPI-anchored proteins. *J. Cell Sci.* **116**, 2149–2155.
- Benedikt, K. (2008) Spatial control of Rho (Rac-Rop) signaling in tip-growing plant cells. *Trends Cell Biol.* **18**, 119–127.
- Berger, J., Howard, A.D., Brink, L., Gerber, L., Hauber, J., Cullen, B.R. and Udenfriend, S. (1988) COOH-terminal requirements for the correct processing of a phosphatidylinositol-glycan anchored membrane protein. *J. Biol. Chem.* **263**, 10016–10021.
- Borner, G.H., Lilley, K.S., Stevens, T.J. and Dupree, P. (2003) Identification of glycosylphosphatidylinositol-anchored proteins in Arabidopsis. A proteomic and genomic analysis. *Plant Physiol.* **132**, 568–577.
- Brady, S.M., Song, S., Dhugga, K.S., Rafalski, J.A. and Benfey, P.N. (2007) Combining expression and comparative evolutionary analysis. The COBRA gene family. *Plant Physiol.* **143**, 172–187.
- Brown, D.M., Zeef, L.A., Ellis, J., Goodacre, R. and Turner, S.R. (2005) Identification of novel genes in Arabidopsis involved in secondary cell wall formation using expression profiling and reverse genetics. *Plant Cell*, **17**, 2281–2295.
- Capron, A., Gourgues, M., Neiva, L.S. *et al.* (2008) Maternal control of male-gamete delivery in Arabidopsis involves a putative GPI-anchored protein encoded by the LORELEI gene. *Plant Cell*, **20**, 3038–3049.
- Chae, K. and Lord, E.M. (2011) Pollen tube growth and guidance: roles of small, secreted proteins. *Ann. Bot.* **108**, 627–636.

- Chatterjee, S. and Mayor, S. (2001) The GPI-anchor and protein sorting. *Cell. Mol. Life Sci.* **58**, 1969–1987.
- Chebli, Y., Kaneda, M., Zerkour, R. and Geitmann, A. (2012) The cell wall of the *Arabidopsis thaliana* pollen tube - spatial distribution, recycling and network formation of polysaccharides. *Plant Physiol.* **160**, 1940–1955.
- Chen, Y.H., Li, H.J., Shi, D.Q., Yuan, L., Liu, J., Sreenivasan, R., Baskar, R., Grossniklaus, U. and Yang, W.C. (2007) The central cell plays a critical role in pollen tube guidance in *Arabidopsis*. *Plant Cell*, **19**, 3563–3577.
- Cheung, A.Y. and Wu, H.M. (2007) Structural and functional compartmentalization in pollen tubes. *J. Exp. Bot.* **58**, 75–82.
- Cheung, A.Y., Wang, H. and Wu, H.M. (1995) A floral transmitting tissue-specific glycoprotein attracts pollen tubes and stimulates their growth. *Cell*, **82**, 383–393.
- Cheung, A.Y., Boavida, L.C., Aggarwal, M., Wu, H.-M. and Feijó, J.A. (2010) The pollen tube journey in the pistil and imaging the in vivo process by two-photon microscopy. *J. Exp. Bot.* **61**, 1907–1915.
- Ching, A., Dhugga, K.S., Appenzeller, L., Meeley, R., Bourett, T.M., Howard, R.J. and Rafalski, A. (2006) *Brittle stalk 2* encodes a putative glycosylphosphatidylinositol-anchored protein that affects mechanical strength of maize tissues by altering the composition and structure of secondary cell walls. *Planta*, **224**, 1174–1184.
- Clough, S.J. and Bent, A.F. (1998) Floral dip: a simplified method for *Agrobacterium*-mediated transformation of *Arabidopsis thaliana*. *Plant J.* **16**, 735–743.
- Eltortza, F., Nuhse, T.S., Foster, L.J., Stensballe, A., Peck, S.C. and Jensen, O.N. (2003) Proteomic analysis of glycosylphosphatidylinositol-anchored membrane proteins. *Mol. Cell. Proteomics*, **2**, 1261–1270.
- Eltortza, F., Mohammed, S., Bunkenborg, J., Foster, L.J., Nuhse, T.S., Brodbeck, U., Peck, S.C. and Jensen, O.N. (2006) Modification-specific proteomics of plasma membrane proteins: identification and characterization of glycosylphosphatidylinositol-anchored proteins released upon phospholipase D treatment. *J. Proteome Res.* **5**, 935–943.
- Frietsch, S., Wang, Y.F., Sladek, C., Poulsen, L.R., Romanowsky, S.M., Schroeder, J.I. and Harper, J.F. (2007) A cyclic nucleotide-gated channel is essential for polarized tip growth of pollen. *Proc. Natl Acad. Sci. USA*, **104**, 14531–14536.
- Fu, Y., Wu, G. and Yang, Z. (2001) Rop GTPase-dependent dynamics of tip-localized F-actin controls tip growth in pollen tubes. *J. Cell Biol.* **152**, 1019–1032.
- Fujita, M. and Kinoshita, T. (2012) GPI-anchor remodeling: potential functions of GPI-anchors in intracellular trafficking and membrane dynamics. *Biochim. Biophys. Acta* **1821**, 1050–1058.
- Galian, C., Bjorkholm, P., Bulleid, N. and von Heijne, G. (2012) Efficient glycosylphosphatidylinositol (GPI) modification of membrane proteins requires a C-terminal anchoring signal of marginal hydrophobicity. *J. Biol. Chem.* **287**, 16399–16409.
- Gao, C., Yu, C.K.Y., Qu, S., San, M.W.Y., Li, K.Y., Lo, S.W. and Jiang, L. (2012) The Golgi-localized *Arabidopsis* endomembrane protein12 contains both endoplasmic reticulum export and Golgi retention signals at its C terminus. *Plant Cell*, **24**, 2086–2104.
- Geitmann, A. (2010) How to shape a cylinder: pollen tube as a model system for the generation of complex cellular geometry. *Sex. Plant Reprod.* **23**, 63–71.
- Gillmor, C.S., Lukowitz, W., Brininstool, G., Sedbrook, J.C., Hamann, T., Poindexter, P. and Somerville, C. (2005) Glycosylphosphatidylinositol-anchored proteins are required for cell wall synthesis and morphogenesis in *Arabidopsis*. *Plant Cell*, **17**, 1128–1140.
- Gomez-Mouton, C., Lacalle, R.A., Mira, E., Jimenez-Baranda, S., Barber, D.F., Carrera, A.C., Martinez, A.C. and Manes, S. (2004) Dynamic redistribution of raft domains as an organizing platform for signaling during cell chemotaxis. *J. Cell Biol.* **164**, 759–768.
- Hewezi, T., Howe, P., Maier, T.R., Hussey, R.S., Mitchum, M.G., Davis, E.L. and Baum, T.J. (2008) Cellulose binding protein from the parasitic nematode *Heterodera schachtii* interacts with *Arabidopsis* pectin methylesterase: cooperative cell wall modification during parasitism. *Plant Cell*, **20**, 3080–3093.
- Higashiyama, T., Yabe, S., Sasaki, N., Nishimura, Y., Miyagishima, S., Kuroiwa, H. and Kuroiwa, T. (2001) Pollen tube attraction by the synergid cell. *Science*, **293**, 1480–1483.
- Hochholdinger, F., Wen, T.J., Zimmermann, R., Chimot-Marolle, P., da Costa e Silva, O., Bruce, W., Lamkey, K.R., Wienand, U. and Schnable, P.S. (2008) The maize (*Zea mays* L.) *roothairless3* gene encodes a putative GPI-anchored, monocot-specific, COBRA-like protein that significantly affects grain yield. *Plant J.* **54**, 888–898.
- Honys, D. and Twell, D. (2004) Transcriptome analysis of haploid male gametophyte development in *Arabidopsis*. *Genome Biol.* **5**, R85.
- Ikezawa, H. (2002) Glycosylphosphatidylinositol (GPI)-anchored proteins. *Biol. Pharm. Bull.* **25**, 409–417.
- Johnson, M.A. and Preuss, D. (2002) Plotting a course: multiple signals guide pollen tubes to their targets. *Dev. Cell*, **2**, 273–281.
- Johnson-Brousseau, S.A. and McCormick, S. (2004) A compendium of methods useful for characterizing *Arabidopsis* pollen mutants and gametophytically-expressed genes. *Plant J.* **39**, 761–775.
- Jones, M.A., Raymond, M.J. and Smirnov, N. (2006) Analysis of the root-hair morphogenesis transcriptome reveals the molecular identity of six genes with roles in root-hair development in *Arabidopsis*. *Plant J.* **45**, 83–100.
- Jürgens, G. (2004) Membrane trafficking in plants. *Annu. Rev. Cell Dev. Biol.* **20**, 481–504.
- Ko, J.H., Kim, J.H., Jayanty, S.S., Howe, G.A. and Han, K.H. (2006) Loss of function of *COBRA*, a determinant of oriented cell expansion, invokes cellular defence responses in *Arabidopsis thaliana*. *J. Exp. Bot.* **57**, 2923–2936.
- Kolsch, V., Charest, P.G. and Firtel, R.A. (2008) The regulation of cell motility and chemotaxis by phospholipid signaling. *J. Cell Sci.* **121**, 551–559.
- Kondoh, G., Tojo, H., Nakatani, Y. et al. (2005) Angiotensin-converting enzyme is a GPI-anchored protein releasing factor crucial for fertilization. *Nat. Med.* **11**, 160–166.
- Lalanne, E., Honys, D., Johnson, A., Borner, G.H., Lilley, K.S., Dupree, P., Grossniklaus, U. and Twell, D. (2004) *SETH1* and *SETH2*, two components of the glycosylphosphatidylinositol anchor biosynthetic pathway, are required for pollen germination and tube growth in *Arabidopsis*. *Plant Cell*, **16**, 229–240.
- Li, Y., Qian, Q., Zhou, Y. et al. (2003) *BRITTLE CULM1*, which encodes a COBRA-like protein, affects the mechanical properties of rice plants. *Plant Cell*, **15**, 2020–2031.
- Li, H.J., Xue, Y., Jia, D.J., Wang, T., Hi, D.Q., Liu, J., Cui, F., Xie, Q., Ye, D. and Yang, W.C. (2011) *POD1* regulates pollen tube guidance in response to micropylar female signaling and acts in early embryo patterning in *Arabidopsis*. *Plant Cell*, **23**, 3288–3302.
- Lu, Y., Chanroj, S., Zulkifli, L., Johnson, M.A., Uozumi, N., Cheung, A. and Sze, H. (2011) Pollen tubes lacking a pair of K⁺ transporters fail to target ovules in *Arabidopsis*. *Plant Cell*, **23**, 81–93.
- Marton, M.L., Cordts, S., Broadhvest, J. and Dresselhaus, T. (2005) Micropylar pollen tube guidance by egg apparatus 1 of maize. *Science*, **307**, 573–576.
- McCormick, S. (1993) Male Gametophyte Development. *Plant Cell*, **5**, 1265–1275.
- McDowell, M.A., Ransom, D.M. and Bangs, J.D. (1998) Glycosylphosphatidylinositol-dependent secretory transport in *Trypanosoma brucei*. *Biochem J.* **335**, (Pt 3) 681–689.
- Obayashi, T., Nishida, K., Kasahara, K. and Kinoshita, K. (2011) ATTED-II updates: condition-specific gene coexpression to extend coexpression analyses and applications to a broad range of flowering plants. *Plant Cell Physiol.* **52**, 213–219.
- Okuda, S., Tsutsui, H., Shiina, K. et al. (2009) Defensin-like polypeptide LUREs are pollen tube attractants secreted from synergid cells. *Nature*, **458**, 357–361.
- Palanivelu, R. and Preuss, D. (2006) Distinct short-range ovule signals attract or repel *Arabidopsis thaliana* pollen tubes *in vitro*. *BMC Plant Biol.* **6**, 7.
- Palanivelu, R., Brass, L., Edlund, A.F. and Preuss, D. (2003) Pollen tube growth and guidance is regulated by POP2, an *Arabidopsis* gene that controls GABA levels. *Cell*, **114**, 47–59.
- Primakoff, P. and Myles, D.G. (2007) Cell-cell membrane fusion during mammalian fertilization. *FEBS Lett.* **581**, 2174–2180.
- Qin, Y., Leydon, A.R., Manziello, A., Pandey, R., Mount, D., Denic, S., Vasic, B., Johnson, M.A. and Palanivelu, R. (2009) Penetration of the stigma and style elicits a novel transcriptome in pollen tubes, pointing to genes critical for growth in a pistil. *PLoS Genet.* **5**, e1000621.
- Roudier, F., Schindelman, G., DeSalle, R. and Benfey, P.N. (2002) The COBRA family of putative GPI-anchored proteins in *Arabidopsis*. A new fellowship in expansion. *Plant Physiol.* **130**, 538–548.

- Roudier, F., Fernandez, A.G., Fujita, M. *et al.* (2005) COBRA, an Arabidopsis extracellular glycosyl-phosphatidyl inositol-anchored protein, specifically controls highly anisotropic expansion through its involvement in cellulose microfibril orientation. *Plant Cell*, **17**, 1749–1763.
- Schindelman, G., Morikami, A., Jung, J., Baskin, T.I., Carpita, N.C., Derbyshire, P., McCann, M.C. and Benfey, P.N. (2001) COBRA encodes a putative GPI-anchored protein, which is polarly localized and necessary for oriented cell expansion in *Arabidopsis*. *Genes Dev.* **15**, 1115–1127.
- Sindhu, A., Langewisch, T., Olek, A., Multani, D.S., McCann, M.C., Vermerris, W., Carpita, N.C. and Johal, G. (2007) Maize *Brittle stalk2* encodes a COBRA-like protein expressed in early organ development but required for tissue flexibility at maturity. *Plant Physiol.* **145**, 1444–1459.
- Sousa, E., Kost, B. and Malho, R. (2008) *Arabidopsis* phosphatidylinositol-4-monophosphate 5-kinase 4 regulates pollen tube growth and polarity by modulating membrane recycling. *Plant Cell*, **20**, 3050–3064.
- Szumanski, A.L. and Nielsen, E. (2009) The Rab GTPase RabA4d regulates pollen tube tip growth in *Arabidopsis thaliana*. *Plant Cell*, **21**, 526–544.
- Tang, W., Kelley, D., Ezcurra, I., Cotter, R. and McCormick, S. (2004) LeSTIG1, an extracellular binding partner for the pollen receptor kinases LePRK1 and LePRK2, promotes pollen tube growth *in vitro*. *Plant J.* **39**, 343–353.
- Tian, G.W., Mohanty, A., Chary, S.N. *et al.* (2004) High-throughput fluorescent tagging of full-length Arabidopsis gene products in planta. *Plant Physiol.* **135**, 25–38.
- Tsukamoto, T., Qin, Y., Huang, Y., Dunatunga, D. and Palanivelu, R. (2010) A role for LORELEI, a putative glycosylphosphatidylinositol-anchored protein, in *Arabidopsis thaliana* double fertilization and early seed development. *Plant J.* **62**, 571–588.
- Wang, W., Wang, L., Chen, C., Xiong, G., Tan, X.Y., Yang, K.Z., Wang, Z.C., Zhou, Y., Ye, D. and Chen, L.Q. (2011) *Arabidopsis* CSLD1 and CSLD4 are required for cellulose deposition and normal growth of pollen tubes. *J. Exp. Bot.* **62**, 5161–5177.
- Wu, H.M., Wong, E., Ogdahl, J. and Cheung, A.Y. (2000) A pollen tube growth-promoting arabinogalactan protein from *Nicotiana glauca* is similar to the tobacco TTS protein. *Plant J.* **22**, 165–176.
- Ye, J., Zheng, Y., Yan, A., Chen, N., Wang, Z., Huang, S. and Yang, Z. (2009) *Arabidopsis* formin3 directs the formation of actin cables and polarized growth in pollen tubes. *Plant Cell*, **21**, 3868–3884.
- Zhang, Y. and McCormick, S. (2007) A distinct mechanism regulating a pollen-specific guanine nucleotide exchange factor for the small GTPase Rop in *Arabidopsis thaliana*. *Proc. Natl Acad. Sci. USA*, **104**, 18830–18835.
- Zhang, Y., He, J. and McCormick, S. (2009) Two Arabidopsis AGC kinases are critical for the polarized growth of pollen tubes. *Plant J.* **58**, 474–484.
- Zhang, Y., He, J., Lee, D. and McCormick, S. (2010) Interdependence of endomembrane trafficking and actin dynamics during polarized growth of Arabidopsis pollen tubes. *Plant Physiol.* **152**, 2200–2210.